

Modelling and Simulation Study of a Wideband Printed Dipole Elliptical Patch Antenna for Sub-6 GHz 5G Spectrum

Gunaram¹, Vijay Sharma², Gaurav Sharma¹, Dharendra Mathur³ and JK Deegwal⁴

¹Department of Physics, Govt. Engineering College, Ajmer -30500

²Department of Physics, Govt. Mahila Engineering College, Ajmer -305002

³Faculty of Nanotechnology, Rajasthan Technical University, Kota, Rajasthan, India - 324010

⁴Department of Electronics and Communication Engg., Govt. Mahila Engineering College, Ajmer -305002

E-mail: ²phyvijay@gmail.com (Corresponding Author)

ABSTRACT

In this article, the modelling and simulation performance of a printed gap coupled dipole elliptical patch antenna (EPA) for the sub-6GHz band of 5G spectrum is presented and verified by fabricated design and measurement results. In prototype design a conventional EPA is transformed into a gap coupled dipole EPA by introducing two horizontal parallel slits along the minor axis. The width and position of the slits are optimized after multiple computations. The fabricated antenna gives rise to a wide impedance bandwidth 2.26-5.50GHz corresponding to -10dB points, which is almost 123.5% for first resonance frequency $f_1 = 2.62\text{GHz}$ and 66.10% for second resonance frequency $f_2 = 4.90\text{GHz}$ with flat gain. The shape and nature of measured radiation patterns of the proposed antenna design within the impedance bandwidth region are similar and stable. Also, the measured and simulated results are in remarkable agreement, which marks the prototype antenna proficient of 5G spectrum coverage in the sub-6GHz band.

Keywords: Sub-6GHz band, 5G spectrum, gap coupled patch antenna, wideband impedance bandwidth, stable radiation pattern

1. INTRODUCTION

5G (fifth generation) is rising as an innovation that will utilize both low (< 1GHz) and high frequencies (1-6GHz and the frequency < 6GHz) in consumer networks referred to as ‘millimeter wave’ frequencies. This assorted spectrum will undoubtedly guarantee the comprehensive coverage at low frequencies, ultra-high speeds (huge diverts in exceptionally high-frequency bands), and low power utilization which is conceived in 5G [1]. Table 1, summarizes the spectrum converge (the key frequency ranges) required for 5G technology.

Table 1. Spectrum Converge with 5G Technology [2]

Sub-1 GHz	1-6 GHz	Above 6GHz
Coverage Layer	Coverage & Capacity Layer	Super Data Layer
Wide area & deep indoor coverage	mMTC (no deep coverage), eMBB, uRLLC	Supports high data rates
mMTC, eMBB, uRLLC		mMTC, eMBB, uRLLC

Here “eMBB stands for Enhanced Mobile Broadband, URLLC stands for Ultra-Reliable Low Latency Communications and mMTC stands for Massive Machine Type Communications”.

According to [3], the “5G mobile communication system has requested a rapid wireless information service to satisfy the high data transfer rate for different applications. The bands

between 3GHz and 5GHz have been advanced for 5G services in numerous nations due to radio wave proliferation and accessible transmission capacity. In USA 3.1-3.55GHz & 3.7-4.2GHz, in Europe 3.4-3.8GHz and in China 3.3-3.6GHz & 4.8-4.99GHz bands have been considered for 5G applications. The consistent inclusion for 5G wireless network has helped the interest of 5G base station antenna with ideal properties, such as wide impedance bandwidth (IBW) with stable radiation pattern and sustained gain”.

Since the inception of microstrip patch antenna (MPA) till the time, it becomes a promising candidate for almost all types of communication devices owing to its appearance assets of lightweight, low-cost easy manufacturing and installation. However, as the IBW of MPA is very small just 2-3%, which makes it unsuitable for modern-day communication devices, as these devices required wide IBW, so that a single antenna may work for various applications simultaneously [4]. Looking these flaws various investigators are trying to enhance the IBW with different techniques and methods that can be found in the open literature, such as the use of thick low permittivity substrate material [5-6], impedance matching network [7], stacked microstrip patches [8], aperture-coupled patches with large slot [9], a capacitive probe feed configuration [10] and arrangement of parasitic radiator nearby the main radiating patch in the same plane [11] etc. The thinking of these practices is to add one or more additional resonances to the MPA configuration.

This technique of parasitically or gap-coupled patches is one of the most successful techniques for bandwidth enhancement. This can be achieved by using coplanar, closely

spaced multiple resonator elements. The logic is that, if the resonant mode of the coupled elements is marginally different to that of the main patch; they may superimpose and at that point, the IBW of the antenna might be enhanced. The control parameters of resonant frequency and IBW are the element of each patch and gap among them. The gap controls the coupling among the patches and along these lines the snugness of the full loop in the impedance locus of the antenna.

Several articles are available that contain the design, analysis, and detailed discussion on gap-coupled or parasitically coupled patches in the open literature. Some of the most cited studies are included here that makes this article easy to understand for the readers. In [12], Kumar and Gupta described this technique where two extra resonators (which are gap-coupled) are integrated into the radiating edges of a rectangular patch microstrip antenna (RPMA) and realized an IBW fivefold of a single RPMA. Further in [13], the authors extended their work, and this time the two added resonators (which are gap-coupled) are integrated to the non-radiating edges, in place of the radiating edges of RPMA. However, in this case, the realized IBW is just doubled of a single RPMA. The study is further extended by placing four additional resonators along the four edges of the patch. The radiation pattern so obtained are also discussed. In [14], Aanandan *et al* presented a compact size monopulse antenna with large bandwidth and less contorted radiation pattern. An improved IBW almost eightfold, contrasted with ordinary single patch antenna is attained by this novel gap coupled microstrip antenna with parasitic elements. Kumar *et al* [15], utilizing the cavity model concept determine the resonant frequency and mode number of gap coupled circular patch microstrip antenna (CPMA) numerically and compared it with the published results in [16]. The results are authenticated by finding the current distribution for full-wave solutions. In [17] Ray *et al* divided RPMA bit by bit into littler components along the width and lengths and by varying the separation, the dual and triple frequency operation can be achieved. The maximum frequency ratio is 1.07 for two strips whereas if the number of elements increases, it increases and becomes 1.19 for five strips.

In [18], Sharma *et al* communicated an assembly of gap coupled elements in elliptical shape that consist of five patches, out of which two pairs of patches have different dimension and placed closed to a truncated ellipse (main patch) backed by a ground plane. By suitably selecting the patch area and gap spacing between gap coupled elements an IBW of 18.5% with presence of circular polarization is attained. Later, Sharma and Sharma [19] extended this concept to a gap coupled assembly (six patches) of RPMA and attained dual-band wide impedance bandwidth antenna for Wi-max application in lower band (2.4–2.69GHz with IBW 11.2%) and upper band (5.25–5.85GHz with IBW 9.7%). In [20], Khanna *et al* presented a modified square fractal MPA with gap coupling and attained an IBW 85.42% concerning the resonant frequency of 1.844GHz. In this structure, the gap coupling and fractal formation are applied simultaneously. In [21], Singh *et al* investigated a L-strip fed compact semi-circular disk MPA with and without shorting pin using the concept of circuit theory. A dual-band behavior is

observed at two different modes *i.e.* 1.3GHz with IBW 6.61% and 6.13GHz with IBW 10.64%. In [22], Singh *et al* proposed an anchor shape antenna employing the concept of parasitic patches and gap coupling. The antenna in anchor shape is converted to its rectangular equivalent (lumped element equivalent) by maintaining the patch area for Wi-max and WLAN applications. Ahmed *et al* [23] discussed a dual-band frequency reconfigurable patch antennas comprises of a left / right-handed transmission line unit cell which is gap coupled to the edge of a radiating RPMA. To achieved a high gain (nearly 12.7dBi), a 2×2 array is also discussed.

On reviewing the literature critically, it is easy to grasp that, use of coplanar parasitic patches can result in large IBW, however, there are a few lacks of utilizing this method. Such as:

- Primarily, to accomplish these sensible bandwidths, wide parasitic components are prerequisites that create the overall size of the antenna arrangement electrically large and due to this, it is hard to build up an array.
- Second, the radiation patterns will in general be mutilated over the range of IBW, due to the absence of symmetry of the created currents about the focus of the antenna.

Perhaps, it is observed that the planar gap-coupling technique is the most effective way to reach broadband operation.

To rectify these issues, the design and simulation study of a wideband gap coupled dual printed EPA is offered in this article for sub-6 GHz, 5G applications. In this structure, the elliptical shape ground plane is not just below the patch, perhaps it is placed aside on the positive x-axis, whereas the patch is along the negative x-axis having two slits at symmetric positions. In the present case, the symmetry of the produced currents about the center of the antenna is maintained as the feed is symmetric to both the coupled patches. At the point, when an extra radiator or radiator has been picked, the point of the antenna architect is to guarantee there is the correct level of connection among these components to improve the performance of the antenna. A significant number of these procedures include modification of feed position and structure of feed element used to energize the antenna.

This article systematically presents the evolution of the presented geometry in the following sections. In the first part, the introduction and literature review is included. In the second section, the design and analysis of an elliptical patch antenna (EPA) are discussed, followed by further modification by placing two horizontal slits in conventional EPA to enrich the IBW. In the third section, to achieve further wider IBW this antenna design is further modified by shifting the ground elliptical patch, such that now it is not just below the patch (as in conventional case) and it gives rise broad IBW of more than 100%. In further sections, the parametric study of the various key factor is discussed along with the discussion on outcomes and concluded at last.

2. ANTENNA DESIGN AND ANALYSIS

2.1 Antenna Configuration

The layout of the printed dipole gap-coupled elliptical patch antenna with horizontal slits is presented in Fig. 1. In this design, a conventional EPA geometry is separated into three patches by the insertion of two parallel narrow slits to the minor axis (x-axis) of EPA as shown in Fig. 1. In this way, the two exterior patches are now gap coupled to the main patch. The dimension size and character of these two exterior patches are identical. Fig. 1 displays the layout of the projected antenna designed on material FR4 with values $\epsilon_r = 4.4$ and loss tangent $\tan\delta = 0.025$. The overall dimension of the presented antenna is $0.24\lambda_0 \times 0.43\lambda_0$, here λ_0 refers to lower edge frequency corresponds to -10dB in S_{11} variation (Fig. 3). The left side elliptical patch (modified) acts as a patch and printed on the top of the substrate surface whereas the right side elliptical patch (conventional) acts as the ground is printed on the bottom side. The dimensions of both the elliptical patches are the same. The feeding point is $(F_d, 0)$. The typical dimensional parameters of the proposed antenna are given in Table 2.

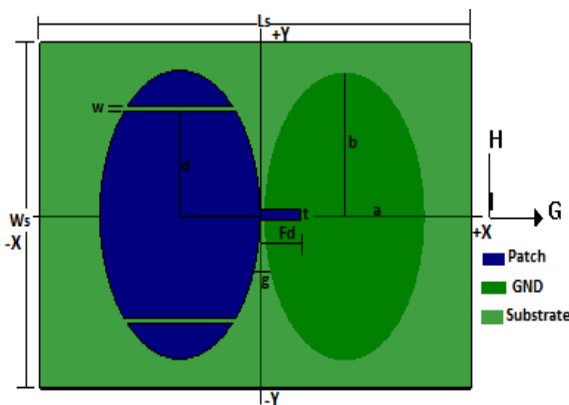


Fig. 1: Layout of the proposed antenna

Table 2. Typical Dimension Parameters for the Proposed Antenna

Parameter	Dimension (mm)
Dimension of semi minor axis 'a' of the radiator patch	10.0
Dimension of semi major axis 'b' of the radiator patch	15.0
Eccentricity value 'e'	0.745
Distance of horizontal slit form origin of ellipse 'd'	11.0
Gap between main patch and coupled patch 'w'	0.7
Gap 'g'	0.5
Length of the feed strip 'Fd'	5.0
Width of the feed strip 't'	1.0
Length of the substrate material 'Ls'	55
Width of the substrate material 'Ws'	30

Table 3. Theoretical, simulated and measured value of resonance for 'antenna 1'

Theoretical	simulated	measured
2.78	2.74	2.78
3.82	3.82	3.81
4.96	4.98	4.98
5.62	5.56	5.60

2.2 Evolution of Antenna Design

In the first step, a conventional EPA named 'antenna 1' is designed, fabricated, and analysed as depicts in Fig. 2(a). The simulation investigation of this 'antenna 1' is carried out by applying the 'Method of Moment' based Zeland IE3D software [24]. A coaxial probe (with probe radius 0.62mm) having 50-ohm impedance is used to energized this fabricated antenna. The S_{11} and gain variation of this 'antenna 1' within frequency range form 2-6GHz is presented in Fig. 3(a). The first four resonances of this 'antenna 1' are observed at 2.78GHz, 3.82GHz, 4.98GHz, and 5.56GHz respectively.

The theoretical analysis of conventional EPA can be perused by solving the wave equation in the elliptical coordinate system. The resonant frequency of elliptical waveguide can be improved and streamlined for the EPA by Rengarajan [25]:

$$f_{11}^{e,o} \text{ (in GHz)} = \frac{15}{\pi a} \sqrt{\frac{q_{11}^{e,o}}{\epsilon_r}} \quad (1)$$

Here $f_{11}^{e,o}$ is the dual resonant frequency of TM_{11}^e and TM_{11}^o mode depends on Mathieu Function $q_{11}^{e,o}$ and 'a' is the physical dimension of semi major axis (in cm). However, generally the measured result of the $f_{11}^{e,o}$ (in GHz) are lesser than calculated values owing to effective (electrical) semi major axis a_{ef} ($a_{ef} > 0$). The a_{ef} is in use to account the energy stored in the fringing field of elliptical edge. Hence, to determine the closed form formula for the $f_{11}^{e,o}$ accurately the physical value of 'a' can be is replaced with the effective value a_{ef} .

For a given mode, it is very rigours to calculate the exact values of Mathieu Function $q_{11}^{e,o}$, that is why in general the approximate Mathieu function $q_{11}^{e,o}$ of the dominant $TM_{11}^{e,o}$ mode are used for calculation-

$$q_{11}^e = -0.0049e + 3.788e^2 - 0.727e^3 + 2.314e^4 \quad (2)$$

$$q_{11}^o = -0.0063e + 0.3831e^2 - 1.1351e^3 + 5.2229e^4 \quad (3)$$

Further, the $f_{11}^{e,o}$ with eccentricities ($e = \sqrt{1 - (\text{minor axis value}/\text{major axis value})^2}$) is analogous to aspect ratios (b/a), subsequently, for the $f_{11}^{e,o}$ formula the effective semi-major axis must be deliberated. The methodology proposed by Kretzschmar [26] is valid to the 'antenna 1' also. The $f_{11}^{e,o}$ of the improved configuration for the TM_{11} mode is premeditated by altering the equation for a circular microstrip antenna [27] as follows:

$$a_{ef} = \left[a^2 + \frac{ha}{0.352\pi\epsilon_r} \left\{ \log\left(\frac{a}{2h}\right) + (1.41\epsilon_r + 1.77) + \frac{h}{a}(0.268\epsilon_r + 1.65) \right\} \right]^{0.5} \quad (4)$$

©2012-21 International Journal of Information Technology and Electrical Engineering

The calculated, simulated and measured value for the first four resonances are tabulated in Table 3 and found in a fairly close match.

In the second step, to increase the IBW of the ‘antenna 1’ (step 1) a couple of narrow parallel slits is inserted in the elliptical patch (parallel to the x-axis) as shown in Fig. 2(b) and named as ‘antenna 2’. These slits separate the main patch and coplanar parasitic patches. After, various optimization the width of slits is fixed at $w=0.7\text{mm}$ and the position of these horizontal slits from the origin of the elliptical patch is kept at $d=11.0\text{mm}$ for simulation and fabrication purpose [28].



Fig. 2(a): Antenna 1



Fig. 2(b): Antenna 2 [26]

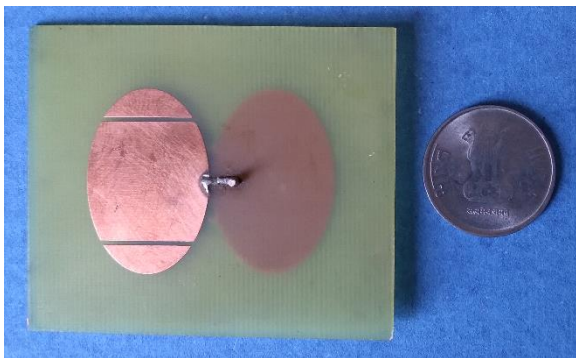


Fig. 2(c): Front view of fabricated antenna structure ‘Antenna 3’



Fig. 2(d): Back view of fabricated antenna structure

Fig. 3(b), presents the S_{11} and gain variation of this ‘antenna 2’ (modified EPA) against frequency. It is perceived that the first two resonance appears at 3.42GHz and 3.68GHz and covers the mid-band of the Wi-Max system with an IBW more than 10%, whereas the third resonance appears in the upper band of Wi-Max at 5.52GHz. It is established that in this

case IBW is increased by almost three times when compared to conventional EPA ‘antenna 1’ (step 1). Still, this achieved IBW is not optimum for many applications used now a day, such as satellite TV requires 12.5% IBW in C-band and 19% IBW for L-band radar, etc [29]. Thus further modification is necessary for this design. To improve the IBW of this ‘antenna 2’ (step 2), further, the efforts are made in the ground to generate extra higher-order mode that may overlap with the fundamental mode of modified EPA.

In the third and final step named as ‘antenna 3’, the ground is shifted right side towards the positive x-axis and is not just below the patch as in step 2. Now in this situation, on one side there is no metal (ground) below the patch and also on the other side, there is no metal (patch) above the ground as shown in Fig. 2(c) and 2(d). However, a dielectric substrate layer is existing with finite dimension $55 \times 30\text{mm}^2$. To energize the patch a feed line of optimum length is connected to patch, which is fed by SMA connector via ground. To grasp the increment in IBW, the comparison of S_{11} (reflection coefficient) variation for different antenna configurations viz ‘antenna1’, ‘antenna2’, and ‘antenna3’ against frequency are plotted in Fig. 3(c). It is easy to understand that for ‘antenna3’ the IBW is extremely large (< 100%) in sub-6 GHz range of 5G spectrum.

3. IMPACTS OF VARIOUS KEY DESIGN FACTORS ON PERFORMANCE OF ANTENNA

With this structure ‘antenna 3’, an enhanced IBW is achieved. For this structure, the key design parameters are the gap among the ground and radiating patch, the position of the slits, and the width of the slits. These parameters are optimized to attain the maximum IBW. The impacts of these parameters on the antenna performance are discussed in this section.

3.1 Effect of Gap (g)

The variation of S_{11} and gain with frequency for various gap values ‘g’ among the ground plane and patch is presented in Fig. 4(a). It is perceived that on increasing the gap value, the extreme end of -10dB on the S_{11} graph shifts towards the lower frequency side and thus reduces IBW. It is perhaps due to the reduction in coupling among the ground and patch. It is also observed that when there is no gap ($g=0$), an optimum IBW is observed with two resonant frequencies 2.72GHz and 4.5GHz. The gain variation shown in the same figure reflects that constant gain is observed for zero gap value, whereas on increasing the gap value the gain for higher frequency reduces.

3.2 Effect of Position of Slits (d)

To optimize the best performance, the position of both the slits is varied with a fixed width value $w=0.5\text{mm}$. The variation of S_{11} and gain in this case with frequency is illustrated in Fig. 4(b). It is found that the maximum IBW is observed for $d = 8.0\text{mm}$. The simulated IBW is 2.92GHz (2.32GHz-5.24GHz), 107.2% concerning first resonance frequency 2.72GHz since in this case one of the resonance mode generated by (dimension of the parasitic patch) is near to one of the resonance mode of the main patch. However, this whole bandwidth cannot be used

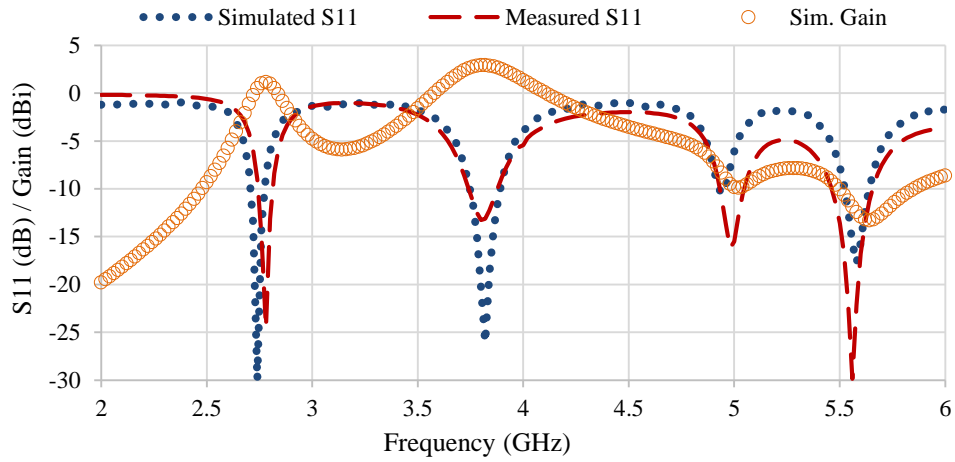


Fig. 3(a): S₁₁ and gain variation of 'antenna1' with frequency

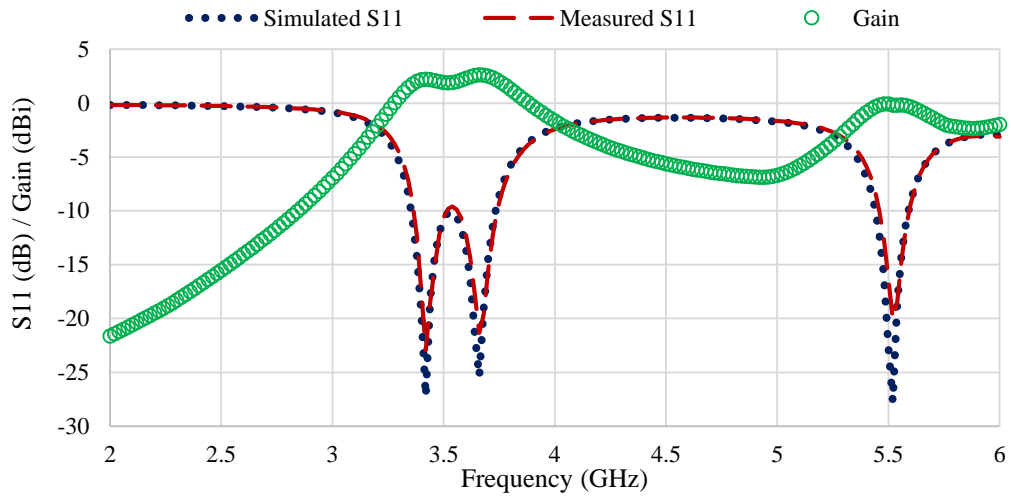


Fig. 3(b): S₁₁ and gain variation of 'antenna2' with frequency

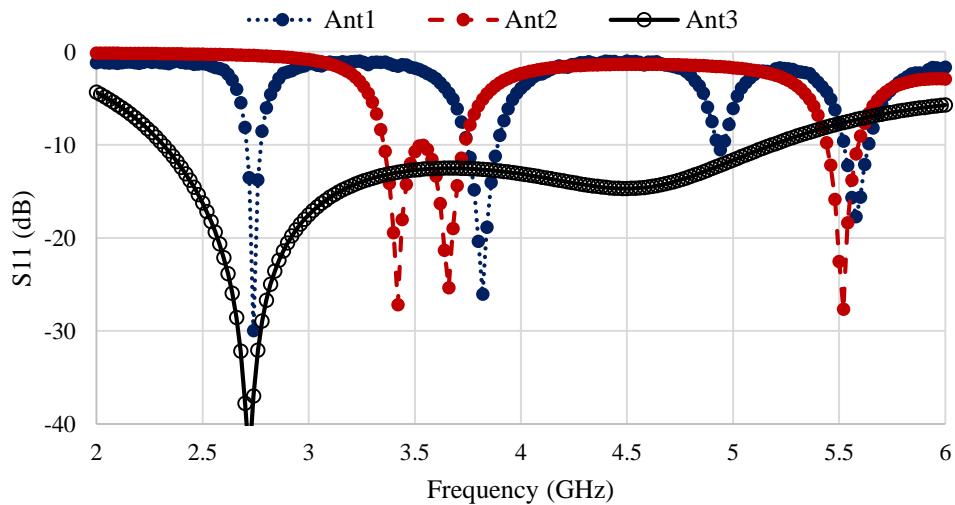


Fig. 3(c): The S₁₁ variation against frequency for 'antenna1', 'antenna2' and 'antenna3'

©2012-21 International Journal of Information Technology and Electrical Engineering

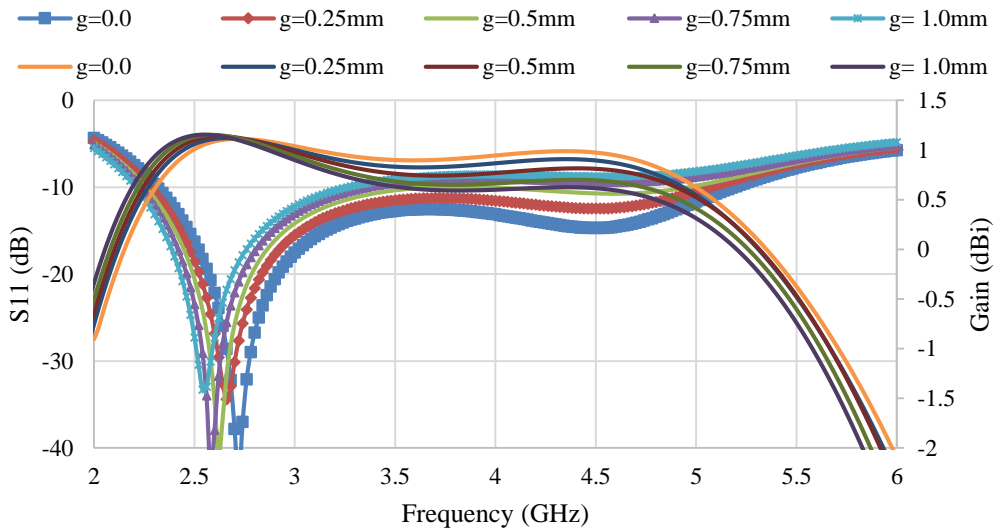


Fig. 4(a): The S_{11} and gain variation with frequency for different gap value 'g' for constant width ($w=0.5\text{mm}$)

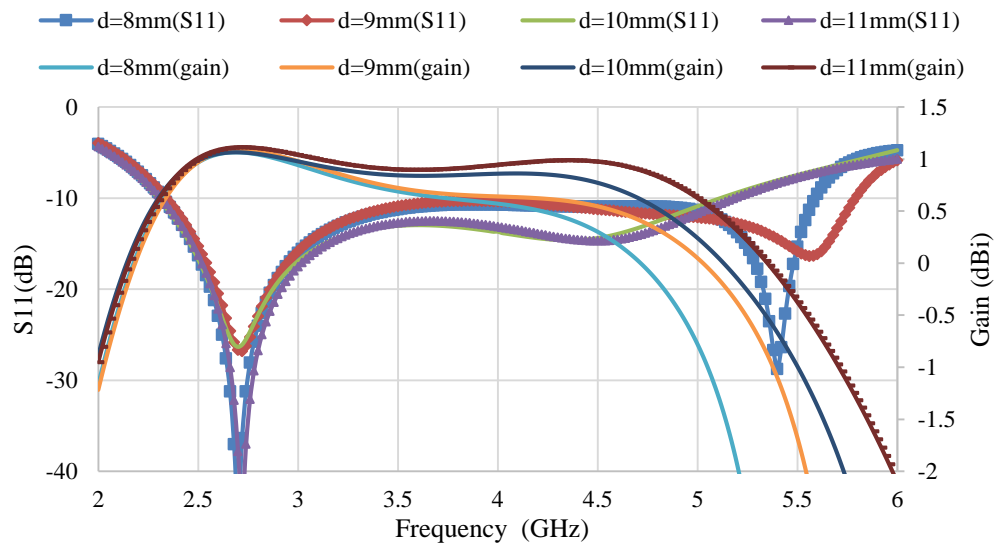


Fig. 4(b): The S_{11} and gain variation with frequency for various slit positions 'd' for constant width ($w=0.5\text{mm}$)

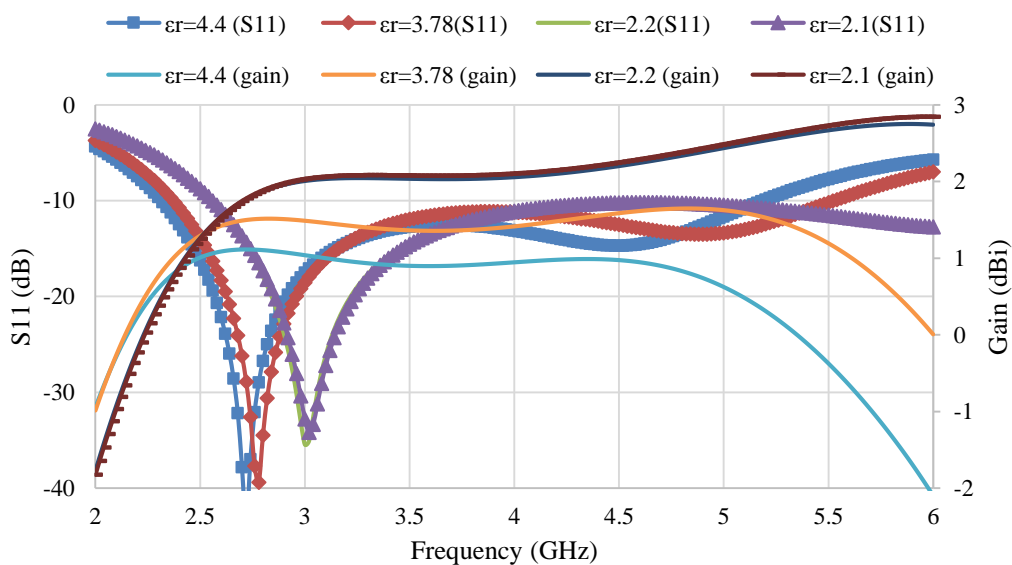


Fig. 4(c): The S_{11} and gain variation for different value of ϵ_r

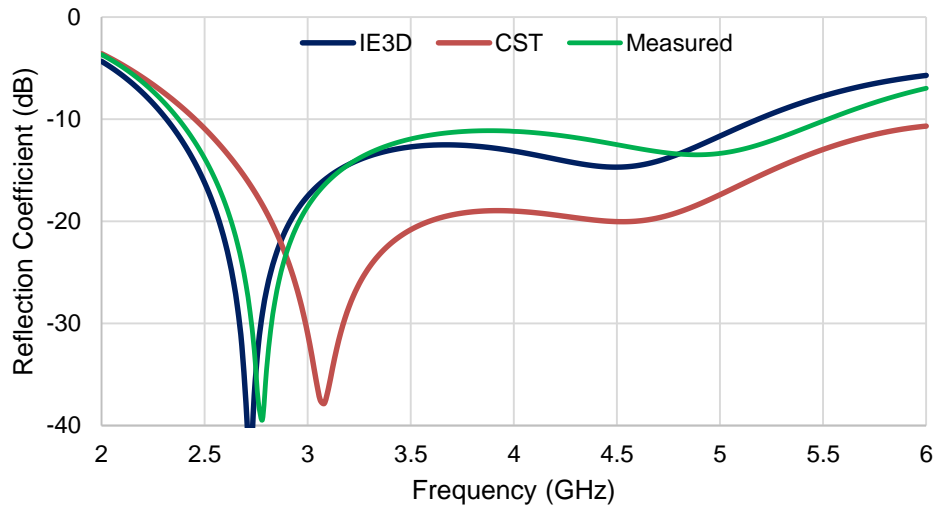


Fig. 5: Comparison of simulated S_{11} (using IE3D and CST) with measured S_{11} for fabricated antenna

practically, as the gain value dropdown to zero at 4.7GHz as shown in Fig. 4(b), it reflects that the useful IBW is just only 67.2%, 2.36GHz (2.32GHz-4.70GHz). However, it can be observed that for $d=11.0\text{mm}$ the gain value is almost steady for frequency ranges from 2.38 to 5.14GHz, which is almost 96.8% about first resonance frequency 2.85GHz and 60.0% pertaining to second resonance frequency 4.60GHz. So, for the purpose of the fabrication of antenna $d=11.0\text{mm}$ is taken.

3.3 Effect of Substrate Permittivity (ϵ_r)

The gain value for the FR-4 substrate used here is quite low due to its lossy nature, however, it can be increased by using some other high-quality substrate materials. To explain this the variation of gain with frequency for several values of dielectric constants is presented in Fig. 4(c). It is observed that for low loss substrate ($\epsilon_r=2.1$) the gain is almost double when compared with FR-4 substrate ($\epsilon_r=4.4$). The variation of S_{11} with frequency for different values of dielectric constant is also presented in Fig. 4(c). It is observed that for the low value of dielectric constant, the increased IBW is observed. This increment in IBW is attributed to the low 'Q' value as the energy stored falls with a low value of ϵ_r .

4. RESULTS AND DISCUSSIONS

To validate the results, firstly the final geometry 'antenna3' is designed and simulated on another electromagnetic simulation tool CST Microwave Studio [30] that uses finite integration technique for simulation. The variation of S_{11} with frequency as attained from IE3D and CST tool is compared with measured result. The S_{11} is measured with available Rohde-Schwarz ZNB VNA as shown in Fig. 5. A slight variation is observed from the results from two tools, this is because of the reason that in CST one has to set the environment before the simulation, whereas, it is not so in IE3D. The measurement result for S_{11} is close to IE3D. The little variation in measured and simulated results is due to the fact that, while designing the geometry in IE3D, the substrate size is considered as infinite (due to the limitation of software edition available), whereas in CST the dimension of the substrate is taken finite.

The simulated IBW is 2.81GHz (2.37GHz-5.18GHz), 103.3% about first resonance frequency 2.72GHz, and 62.4% relating to second resonance frequency 4.50GHz, whereas the measured IBW is 2.40-5.51GHz, which is almost 111.8% relating to first resonance frequency 2.78GHz and 63.4% about second resonance frequency 4.90GHz.

As per the definition of bandwidth, the radiation pattern and other characteristic parameters of antenna such as directivity and gain should be stable within this IBW range (corresponds to -10dB). To validate the radiation characteristics of the proposed antenna, the radiation patterns are measured in the anechoic chamber as shown in Fig. 6.

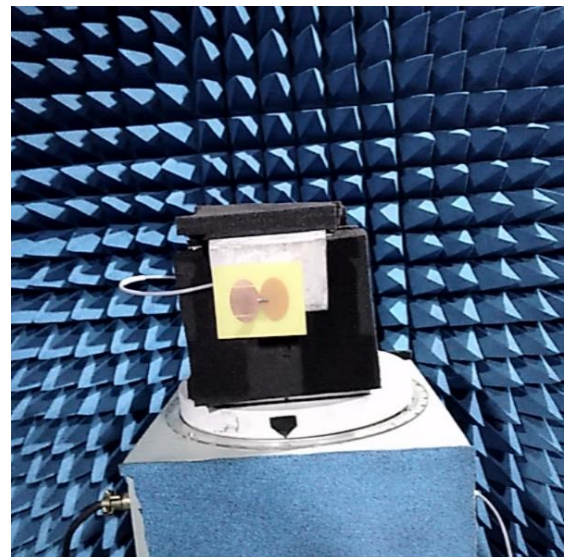


Fig. 6: Fabricated antenna in anechoic chamber for radiation pattern measurement

The simulated and measured radiation pattern of fabricated antenna for both the resonances 2.62GHz and 4.90GHz for $\phi = 0$ deg (xz-plane) and $\phi = 90$ deg (yz-plane) is displayed in Fig. 7 (a, b) and Fig. 8(a, b). It is observed that for in $\phi = 0$ deg (xz-plane) the patterns have a shape of eight i.e. 'dumbbell like' and the direction of maximum radiation is towards $\theta = 0^\circ$ that is normal to patch, and $\theta = 180^\circ$ that is in opposite direction,

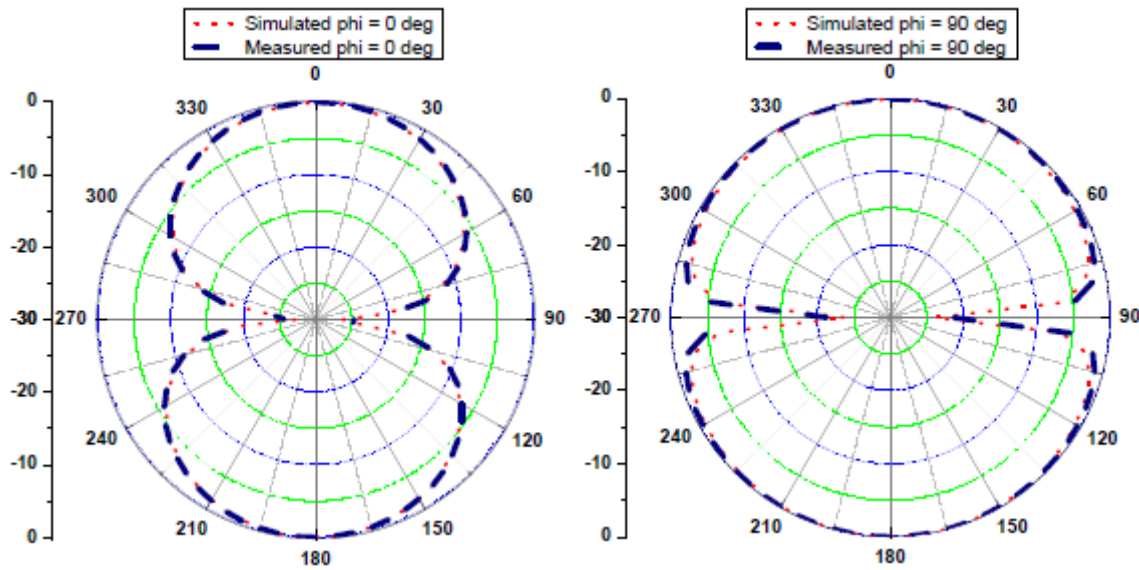


Fig. 7(a, b): Radiation pattern (simulated + measured) at resonant frequency 2.62GHz in (a) xz-plane ($\phi = 0$ degree) and (b) yz-plane ($\phi = 90$ degree)

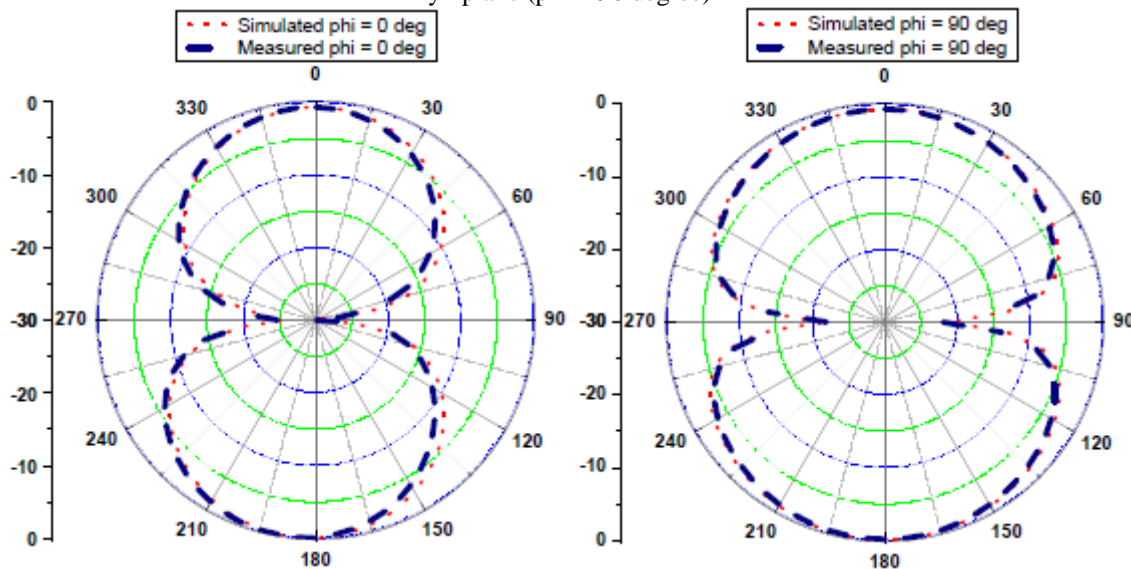


Fig. 8(a, b): Radiation pattern (simulated + measured) at resonant frequency 4.90GHz in (a) xz-plane ($\phi = 0$ degree) and (b) yz-plane ($\phi = 90$ degree)

which is the required parameters for an antenna for practical application. For $\phi = 90$ deg (yz-plane) the shape of patterns is nearly omnidirectional. For two resonances the direction of 3dB beamwidth is (0, 0) degree and (47.43, 129.68) degree. In all, it is found that the E-plane radiation patterns are more directional than the H-plane radiation patterns.

To examine and validate this the variation of gain simulated and measured with frequency is displayed in Fig. 9. Both the traces are fairly matched and variation of gain within -10dB points are within 0.5dBi. It shows that gain value is low, however, it is sustained in the required frequency range.

The various antenna parameter values like efficiency (radiation and antenna), gain and directivity of the prototype antenna is given in Table 4. The direct relation between directivity and antenna efficiency is expressed as per relation

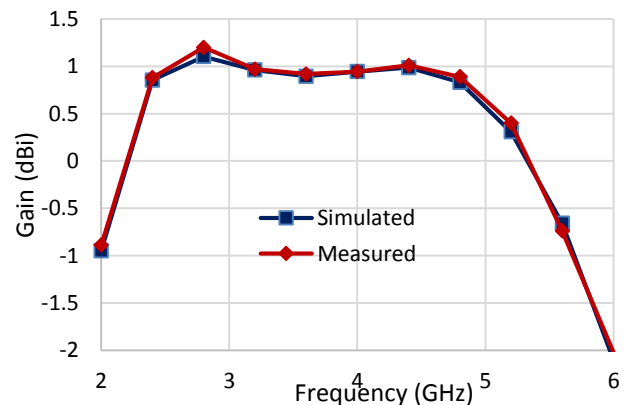


Fig. 9: Measured and simulated deviation of gain for fabricated antenna with frequency

©2012-21 International Journal of Information Technology and Electrical Engineering

$G = \eta D$. Here η is the antenna efficiency factor which is dimensionless. For a lossless antenna $\eta = 1$ and gain will be the same as the directivity. However, in practice, gain is always a smaller amount than the directivity D as replicates from Table 4.

The performance of the proposed work is compared with articles published recently in the referred journal on dual/wideband antennas and presented in Table 5. It can be

perceived that the projected antenna offers an extended IBW in comparison to the published work with low volume size. Perhaps, the volume of Ref. [34] is less in comparison to the proposed work but at the cost of IBW as it is only 71%. The gain value for Ref. [35 & 36] is nearly 8dBi which is sufficiently high in comparison to offered antenna at the cost of size.

Table 4. Typical Antenna Parameters for Printed Dipole Gap-Coupled EPA With Horizontal Slits

Parameter	f_1	f_2	f_l	f_h
Frequency (GHz)	2.62	4.90	2.26	5.60
Impedance Bandwidth (%)	105.8	64	-	-
Radiation Efficiency (%)	67.35	55.47	70.3	47.8
Antenna Efficiency (%)	67.08	50.77	65.7	41.2
Gain (dBi)	1.23	1.26	0.91	0.73
Directivity (dBi)	2.96	4.21	2.72	4.58
3dB Beam Width Degree	(0, 0)	(47.4321, 129.678)	(0, 0)	(41.3732, 114.916)

Table 5. Performance Comparison of Previously Published Dual/Wide Band Antennas with Proposed Work

Reference	Material	BW % (range in GHz)	Size (mm × mm × mm)	Volume (mm ³)
31	FR-4	63.97% (1.93–3.745)	60.0 × 50.0 × 1.58	4740
32	FR-4	10.3% (5.43-6.02) and 45.16% (8.4-13.3)	30.0×30.0×3.2	2880
33	PTFE	27 % (4.5-5.6)	46.0×38.0 × 1.58	2762
34	FR-4	71% (1.9 -3.6)	35.0 × 35.0 × 1.58	1936
35	FR4	67.50%, (2.75-5.45)	130 × 130 × 10	169000
36	FR4	56.87% (2.97-5.33)	100 × 100 × 1.6	6000
Proposed Work	FR-4	123.5% (2.26-5.50)	55×30×1.6	2640

5. CONCLUSION

The design, analysis, and experimental results of a wideband dual-frequency printed gap-coupled dipole elliptical patch antenna having a couple of parallel narrow slits are presented in this article. To understand the mechanism initially the performance of conventional EPA is discussed and thereafter to conceive the desired results the modification in this antenna geometry is incorporated. The presented prototype antenna gives rise to a wide measured IBW, which is 3.24GHz (2.26GHz-5.50GHz), 123.5% relating to first resonance frequency 2.62GHz and 66.10% corresponding to the second resonance frequency. However, the useful IBW is lesser than these values, because the gain is not stable for full IBW range. The useable IBW is nearly 96.0%. The radiation pattern, gain and directivity values are tabulated for well understanding of results. All these values are found to be as per the desired standard. Measured results are found in great agreement with results attained from simulation software, which mark the offered design promising in multimedia applications. Since the offered prototype antenna covers the sub-band 2–6GHz for 5G applications, it may be useful in mobile TV, satellite radio, wireless LAN-802.11b, and 802.11g.

ACKNOWLEDGEMENTS

Authors are thankful to Competitive Research Scheme by RTU (ATU) TEQIP III (project ID TEQIP-III/RTU(ATU)/CRS/2019-20/64) and TEQIP Collaborative

Research Scheme by NPIU and AICTE (CRS ID 1-5763895962) for supporting this work.

REFERENCES

- [1] <https://gsacom.com/5g-spectrum-bands/>. 2019.
- [2] A White Paper on Enabling 5G in India. 22nd February 2019. https://main.trai.gov.in/sites/default/files/White_Paper_22022019.pdf
- [3] D. A. Rahman, S.Y. Mohamad, N.A. Malek and S.M. Zabri, "A wideband mm-wave printed dipole antenna for 5G applications". *Indonesian Journal of Electrical Engineering and Computer Science*, vol. 10, no. 3, pp. 943-950, 2018.
- [4] Gunaram and V Sharma, Microstrip Antenna-inception, Progress and Current-state of The Art Review, Recent Advances in Electrical & Electronic Engineering, vol. 13, no. 6, pp. 769 – 794, 2020. doi : 10.2174/2352096513666200110151616
- [5] T. Firmansyah, H. Suhendar, R. Wiryadinata, M. Iman Santoso, Y. R. Denny, T. Supriyanto, "Bandwidth and gain enhancement of MIMO antenna by using ring and circular parasitic with air-gap microstrip structure". *TELKOMNIKA*, vol. 15, no. 3, pp. 1155-1163, 2017.
- [6] Vijay Sharma, V.K. Saxena, J.S. Saini, D. Bhatnagar, K.B. Sharma, D. Pal, L.M. Joshi, "Wide band dual frequency right triangular microstrip antenna with parallel narrow slits", *International Journal of Microwave and Optical Technology Letters*, vol. 52, pp. 1082-1087, 2010. doi: 10.1002/mop.25113
- [7] K. L. Wong, "Compact and Broadband Microstrip Antennas", John Wiley & Sons, New York, NY, USA, 2003.
- [8] Gunaram, V Sharma, S. Shekhawat, Pawan Jain and J. K. Deegwal, Coaxial feed dual wideband dual polarized stacked

©2012-21 International Journal of Information Technology and Electrical Engineering

- microstrip patch antenna for S and C band communication, AIP Conference Proceedings 2220, Issue 1, 130067 2020. <https://doi.org/10.1063/5.0001646>
- [9] S. Soodmand, "Circular formed dual-band dual-polarized patch antenna and a method for designing compact combined feed networks" *International Journal of Electronics and Communications*, vol. 65, no.5, pp. 453-457, 2011.
- [10] Veeresh G. Kasabegoudar, Dibyant S. Upadhyay, K. J. Vinoy, "Design studies of ultra-wideband microstrip antennas with a small capacitive feed", *International Journal of Antennas and Propagation*, Article ID 67503, 8 pages, 2007. doi:10.1155/2007/67503
- [11] Vijay Sharma, "A novel design of parasitically gap coupled patches forming an elliptical patch antenna for broadband performance", *Chinese Journal of Engineering*, Article ID 365048, 6 pages 2014. doi:10.1155/2014/365048.
- [12] G. Kumar, K. Gupta, "Broad-band microstrip antennas using additional resonators gap-coupled to the radiating edges", *IEEE Transactions on Antennas and Propagation*, vol. 32, pp. 1375-1379, 1984. doi: 10.1109/TAP.1984.1143264
- [13] G. Kumar, K. Gupta, "Nonradiating edges and four edges gap-coupled multiple resonator broad-band microstrip antennas", *IEEE Transactions on Antennas and Propagation*, vol. 33, pp. 173-178, 1985. doi: 10.1109/TAP.1985.1143563
- [14] C. K. Aanandan, P. Mohanan, K. G. Nair, "Broad-band gap coupled microstrip antenna", *IEEE Transactions on Antennas and Propagation*, vol. 38, pp. 1581-1586, 1990. doi: 10.1109/8.59771
- [15] P. Kumar, T. Chakravarty, G. Singh, S. Bhooshan, S. K. Khah, A. De, "Numerical computation of resonant frequency of gap coupled circular microstrip antennas", *J. of Electromagnetic Waves and Applications*, vol. 21, pp.1303-1311, 10, 2007.
- [16] K. P. Ray, G. Kumar, "Multi-frequency and broadband hybrid coupled circular microstrip antennas", *Electronics Letters*, vol. 33, pp.437-438, 1997.
- [17] K. P. Ray, V. Sevani, R. K. Kulkarni, "Gap coupled rectangular microstrip antennas for dual and triple frequency operation", *Microwave and Optical Technology Letters*, vol. 49, pp. 1480-1486, 2007. doi:10.1002/mop.22452
- [18] V. Sharma, K. B. Sharma, V. K. Saxena, D. Bhatnagar, "Radiation performance of circularly polarized broadband gap coupled elliptical patch antenna", *Frequenz*, vol. 66, pp. 69-74, 2012. doi:10.1515/freq-2012-0018.
- [19] V. Sharma, M. M. Sharma, "Wideband gap coupled assembly of rectangular microstrip patches for wi-max applications", *Frequenz*, vol. 68-2, pp. 25-31, 2014. doi:10.1515/freq-2013-0053.
- [20] A. Khanna, D. K. Srivastava, Jai Prakash Saini, "Bandwidth enhancement of modified square fractal microstrip patch antenna using gap-coupling", *International Journal of Engineering Science and Technology*, vol. 182, pp. 286-293, 2015. doi:10.1016/j.jestch.2014.12.001
- [21] A. Singh, J. A. Ansari, Kamakshi, M. Aneesh, S. S. Sayeed, "L-strip proximity fed gap coupled compact semi-circular disk patch antenna" *Alexandria Engineering Journal*, vol. 53, no. 1, pp. 61-67, 2014. doi:10.1016/j.aej.2013.12.001
- [22] Vivek Singh, Brijesh Mishra, Rajeev Singh, "Anchor shape gap coupled patch antenna for WiMAX and WLAN applications", *COMPEL - The International Journal for Computation and Mathematics in Electrical and Electronic Engineering*, vol. 38, pp.263-286, 2019, doi:10.1108/COMPEL-12-2017-0546
- [23] Z. Ahmed, M. M. Ahmed, M. B. Ihsan, A. A. Chaudhary, J. K. Arif, "Novel dual band patch antenna with Gap coupled composite right/left-handed transmission line" *International Journal of Microwave and Wireless Technologies*, pp.1-7, 2018. doi:10.1017/s1759078718001162.
- [24] <https://www.rfglobalnet.com/doc/full-wave-3-d-em-simulator-for-both-planar-an-0001>. 2019.
- [25] S. R. Rengarajan, "Resonance frequency of elliptical microstrip antennas", *Electronics Letters*, vol. 29, pp. 1066-1067, 1993. doi: 10.1049/el:19930712
- [26] J. G. Kretzschmar, "Wave propagation in hollow conducting elliptical waveguides", *IEEE Transactions on Microwave Theory and Techniques*, vol. 18, pp. 547-554, 1970. doi: 10.1109/TMTT.1970.1127288
- [27] Ramesh Garg, Prakash Bhartia, Inder Bahl, and Apisak Ittipihoon, "Microstrip Antenna Design Handbook", Artech House, 875 pages ISBN 0-89006-513-6, 2001.
- [28] V. Sharma, V. K. Saxena, J. S. Saini, D. Bhatnagar, K. B. Sharma, L. M. Joshi, "Broadband gap-coupled assembly of patches forming elliptical patch antenna", *Microwave and Optical Technology Letters*, vol. 532, pp. 340-344, 2010. doi:10.1002/mop.25693.
- [29] G. Kumar, K. P. Ray, "Broadband Microstrip Antennas", Artech House, London, UK, pp. 199, 2003.
- [30] <https://www.cst.com/>. 2019.
- [31] R. K. Saini and S. Dwari, "CPW-fed broadband circularly polarized rectangular slot antenna with L-shaped feed line and parasitic elements". *Microw. Opt. Technol. Lett.*, vol. 57, no. 8, pp. 1788-1794, 2015.
- [32] A. H. Majeed and K.H. Sayidmarie, "Extended-bandwidth microstrip circular patch antenna for dual band applications", *International Journal of Electrical and Computer Engineering*, vol. 8, no. 2, pp. 1056-1066, 2018.
- [33] K. Mandal, S. Sarkar and P.P. Sarkar, "Bandwidth enhancement of microstrip antennas by staggering effect" *Microw. Opt. Technol. Lett.*, vol. 53, no.10, pp. 2446-2447, 2018.
- [34] Z. Erreguig Z and H. Ammor, "A miniature broadband microstrip antenna for LTE. Wi-Fi and WiMAX applications", *International Journal of Electrical and Computer Engineering*, vol. 8, no. 6, pp. 5238-5244, 2018.
- [35] Bei Huang, Weifeng Lin, Jialu Huang, Jun Zhang, Gary Zhang and Fugen Wu, "A patch/dipole hybrid-mode antenna for sub-6GHz communication", *Sensors* 2019, 19, 1358; doi:10.3390/s19061358
- [36] Bei Huang, Mochao Li, Weifeng Lin, Jun Zhang, Gary Zhang, Fugen Wu, "A compact slotted patch hybrid-mode antenna for sub-6 GHz communication", *International Journal of Antennas and Propagation*, vol. 2020, Article ID 8262361, 8 pages, 2020. <https://doi.org/10.1155/2020/8262361>

AUTHOR PROFILES



Dr Gunaram has done his B.Sc. and M.Sc. in Physics from JNV University, Jodhpur, India and Ph.D. from Bhagwant University, Ajmer India in 2020. Currently he is working in Department of Physics, Government Engineering College, Ajmer (India) and perusing for his PhD Degree at Bhagwant University, Ajmer (India). He has authored several reserach article in field of patch antenna. His reserach intereset include design and analysis of patch antennas for modern communication system. He has a research project funded by AICTE on 4G antennas.

©2012-21 International Journal of Information Technology and Electrical Engineering



Vijay Sharma completed his UG, PG, and doctoral research in Physics from the University of Rajasthan, Jaipur (India) in the year 2000, 2002, and 2011 respectively. His research interest includes the design and development of compact size circular polarized antenna, the wideband antenna with high gain for wireless communication, and other applications.

He has more than 17 years of teaching and research experience. Currently, he is working as Assistant Professor, in the Department of Physics, Government Mahila Engineering College, Ajmer (India). He has authored more than 35 research articles in various reputed journals and conferences.

He is a life member of the Indian Physics Association, Indian Association of Physics Teachers, and International Association for the Engineers. He is the reviewer of many prestigious journals including Bentham Science, Electronics Letters, and IET MAP. Currently, he is working on two projects first design and analysis of some novel patch antenna geometry for fifth-generation wireless (5G) communications, and the other one is the design and development of patch antennas for modern-day IoT applications.



Dr. Gaurav Sharma has done his B.Sc. and M.Sc. in Physics from Delhi university and completed his doctoral research from the pioneer research institute in the accelerator physics "Inter university accelerator centre" while registered at DTU. He has more than 10 publications in

the reputed journals which include Physics letter A and European journals of Physics. He has been awarded with the JRF during his doctoral and received Commendable Research Award by the Delhi Technological University for the year

2016-17. He has been working as assistant professor (NPIU) since 2018 at Engineering College, Ajmer, India. Currently he is working on MPA for LTE project under Collaborative Research Scheme from NPIU and AICTE.



Dr. Dharendra Mathur is currently working as a full Professor at Rajasthan Technical University, Kota, India he has completed his M.E (Master of Engineering) from (BITS, Pilani and Ph. D from MNIT, Jaipur, India. He has morethan 28years of teaching and research experieence . He has authored more than 40reserch articles in various

Journal and conference of international repute. His current research area of interest includes design and testing of 5G antenna and Nano antennas.



Dr. J. K. Deegwal is an Associate Professor and Head in Deaprtment of Electronics and Instrumentation Engineering at Government Engineering College, Ajmer (India). He has more than 25 yrs of teaching and research. Currently he is working as a Principal of Government

Mahila Engineering College, Ajmer (India). He has guided three PhD Scholor in field of antenna engineering. He is also associated with mutiple projects related to development of patch antennas and wireless communication systems.